DC to 40-GHz Compact Single-Layer Crossover

Ali Tajik, Mohammad Fakharzadeh, *Senior Member, IEEE*, and Khashayar Mehrany

***Abstract*— In this letter, a compact, wideband, and fully planar microstrip crossover structure is proposed. This design is based on a compact microstrip to coplanar waveguide transition, which has a measured bandwidth extending from dc to 40 GHz. At 20 GHz, the measured insertion loss, return loss, and isolation are better than 0.35, 21, and 19 dB, respectively. This circuit is ultracompact with the core size of 3 mm × 3 mm, which is 0.2λ × 0.2λ at 20 GHz.**

***Index Terms*— Compact design, crossover, microstrip to coplanar waveguide (CPW) transition, millimeter-wave, packaging, single layer, wideband.**

I. Introduction

SINGLE-layer packaging decreases the packaging cost and fabrication time, as well as heat exchange issues, significantly. A key element in a single-layer package is the crossover, where two microstrip lines pass over each other. A proper crossover must have a low insertion loss, high isolation between paths, compact size, and large bandwidth.

In some early works, an air bridge is used to design a crossover [1]. In this letter, two capacitors are used to compensate the inductance of wire-bonds. Although the structure has an acceptable return loss and wide operation bandwidth (0–12 GHz), the complicated fabrication process is a disadvantage. Moreover, the coupling between two paths is not reported. Besides, there are coupler-based planar crossovers [2]–[4], which are not usually wideband. In [3], a crossover with several sections of branch-line couplers is proposed to improve bandwidth. The simulated bandwidth of the crossover with three and four coupler sections are 22% and 33% bandwidth, respectively, where the bandwidth is improved with the price of increasing the size and insertion loss. A crossover consisting of a ring and two orthogonal sections is proposed in [2]. Furthermore, a compact crossover using lumped elements with 20% bandwidth is proposed in [5].

In [6], a new microstrip to coplanar waveguide (CPW) transition is employed to use both sides of the board for crossover design. Nevertheless, the large dimension of patches on both sides of substrate can cause radiation loss, especially at high frequencies. Moreover, this design does not cover the frequencies below 3 GHz. In [7], the operating bandwidth of the crossover has significantly increased (dc 6 GHz) but a large area is occupied by vias.

Manuscript received March 20, 2018; revised April 29, 2018; accepted May 22, 2018. Date of publication June 13, 2018; date of current version August 7, 2018. *(Corresponding author: Mohammad Fakharzadeh.)*

The authors are with the Electrical Engineering Department, Sharif University of Technology, Tehran, Iran (e-mail: ali.tajik@ee.sharif.edu; fakharzadeh@sharif.edu; mehrany@sharif.edu).

Color versions of one or more of the figures in this paper are available online at http://ieeexplore.ieee.org.

Digital Object Identifier 10.1109/LMWC.2018.2843134

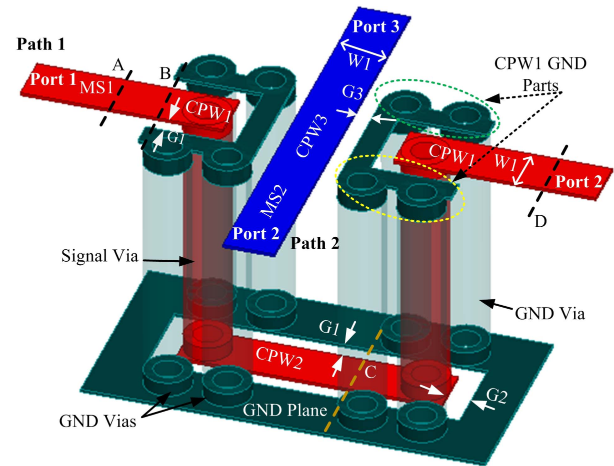

Fig. 1. 3-D view of the proposed crossover structure.

Considering the drawbacks of the previous designs, in this letter, a new planar crossover structure based on CPW-microstrip-CPW transition is proposed and measured for dc to millimeter-waveband operation, which is very compact and relatively low-loss.

II. Design of the Proposed Crossover

The proposed structure for the wideband crossover is illustrated in Fig. 1, which consists of two paths and four ports. Path 2 is placed completely on the top metal layer of the substrate, but path 1 bridges path 2 using the bottom layer. Path 1 starts with a 50-Ω microstrip line (MS1) followed by a CPW line (CPW1) with the same width as microstrip section. CPW1 is connected to the bottom layer through a via (signal via) with a diameter equal to the linewidth. Signal via, connects CPW1 to another CPW line (CPW2) on the bottom layer. The ground part of CPW1 is connected to the ground layer of the structure, with ground vias. Without it, CPW1 is neither a CPW line nor a microstrip line because the ground plane under this section is removed to open space for crossover structure (G2 gap). Fig. 2 illustrates the role of this section in improving the path 1 impedance. Fig. 2(a) and (b) shows the crossover with and without the horizontal ground section, respectively. Fig. 2(c) and (d) compares the electric field concentration around signal via in these two cases. As discussed in [8], the ground vias in Fig. 2(a) form a quasi-coaxial section, which confines the fields around signal via, resulting in a better impedance matching. Fig. 2(e) compares the reflection coefficient of these two designs. It is seen that the extended ground section improves the impedance matching significantly, e.g., 18.5 dB at 10 GHz and 12.5 dB at 36 GHz.

1531-1309 © 2018 IEEE. Personal use is permitted, but republication/redistribution requires IEEE permission.
See http://www.ieee.org/publications_standards/publications/rights/index.html for more information.

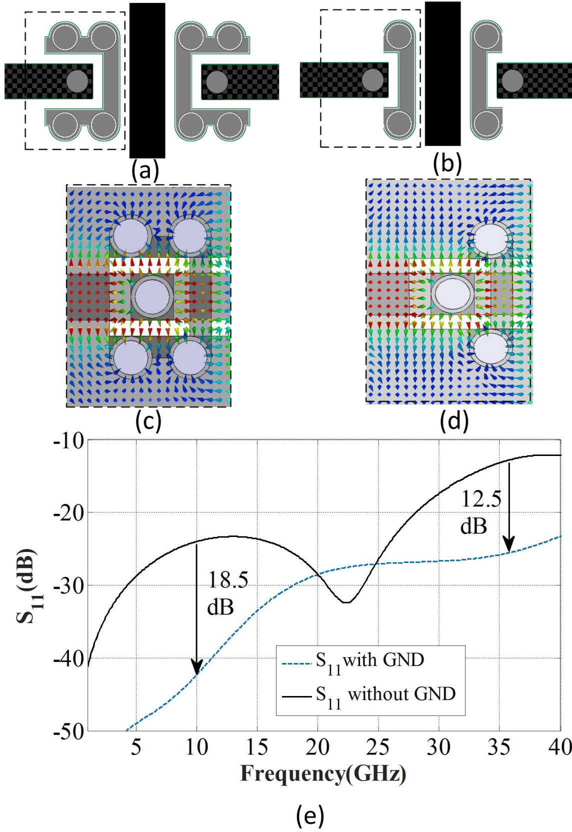

Fig. 2. Top view of the crossover structure. (a) CPW1 with horizontal GND section. (b) CPW1 without GND section. (c) E-field concentration of (a). (d) E-field concentration of (b). (e) S_{11} of path 1 for both designs.

Path 2 of the crossover starts by a 50-Ω microstrip section (MS2), which converts to CPW (CPW3) with the same width to reduce coupling between paths. The ground section of CPW3 is connected to the ground of the structure by GND vias. Path 2 is terminated by a 50-Ω microstrip section.

A. Microstrip to CPW Transition

Fig. 1 shows the main design parameters for this crossover, including line widths and gap sizes. The substrate used in this letter is RO4003 with $\epsilon_r = 3.6$, $\tan\delta = 0.0027$, and 8 mil thickness. The corresponding 50-Ω linewidth, $W1$, is 17 mil.

The critical component of path 1 is the transition from MS1 to CPW1, which is characterized by $W1$ and $G1$. Fig. 3(a) shows the simulated reflection coefficient (S_{11}) when W1 is constant (425 μm) and G1 is swept to vary the impedances of CPW1 and CPW2 lines. According to the results, the best matching is achieved when G1 is around 150 μm.

Similarly, Fig. 3(b) shows the impedance matching for path 2 when G3 is swept from 30 to 150 μm and G1 is kept constant (150 μm). It is seen that the best impedance matching is achieved by choosing G3 as 100 μm.

To illustrate the conversion of the microstrip electrical fields to CPW mode, Fig. 4 displays the electric field concentration at different cross sections (A, B, C, and D lines shown in Fig. 1) of the path 1, which show the correct conversion of CPW to microstrip modes and vice versa.

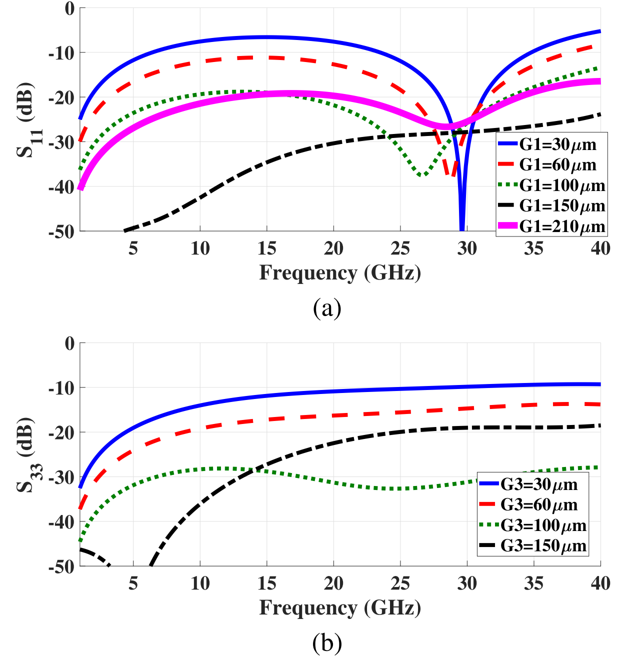

Fig. 3. Simulated impedance matching of (a) path 1 and (b) path 2 for different values of the CPW gap.

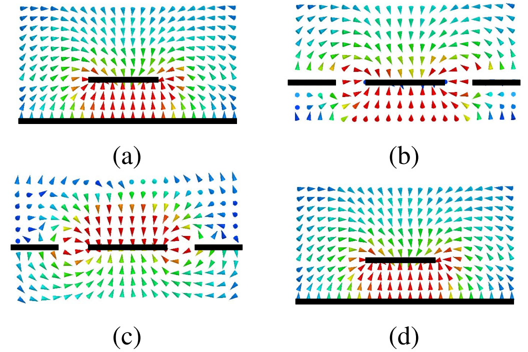

Fig. 4. Electrical fields on (a) plane A (microstrip), (b) plane B (CPW), (c) plane C (CPW), and (d) plane D (microstrip) on path 1. Black thick lines: conductors.

B. Effect of Substrate Thickness

To investigate the effect of the substrate thickness on the crossover bandwidth, the crossover is optimized for the different thickness values to achieve the largest bandwidth. The bandwidth of the structure decreases as the thickness is increased. The achieving bandwidth values of the structure are 50, 43, 26, and 16 GHz for the thickness of 8, 12, 20, and 32 mil, respectively. The bandwidth of the structure is mainly affected by the reflected power in the first path. As the thickness of the structure increases, the height of the signal via is increased, thus at higher frequencies, it radiates and degrades the return loss of path 1.

III. Simulation and Measurement Results

The structure is designed and fabricated in 8-mil RO4003 substrate, shown in Fig. 5. The linewidth (W1) is 17 mil for 50-Ω line, and G2 is 200 μm (obtained from optimization). Diameter of all vias is equal to 0.4 mm. As noticed in Fig. 3, the best values of G1 and G3 are 150 and 100 μm,

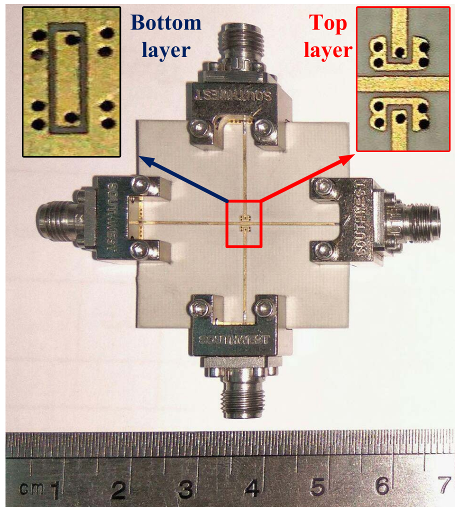

Fig. 5. Fabricated wideband crossover with K-type connectors.

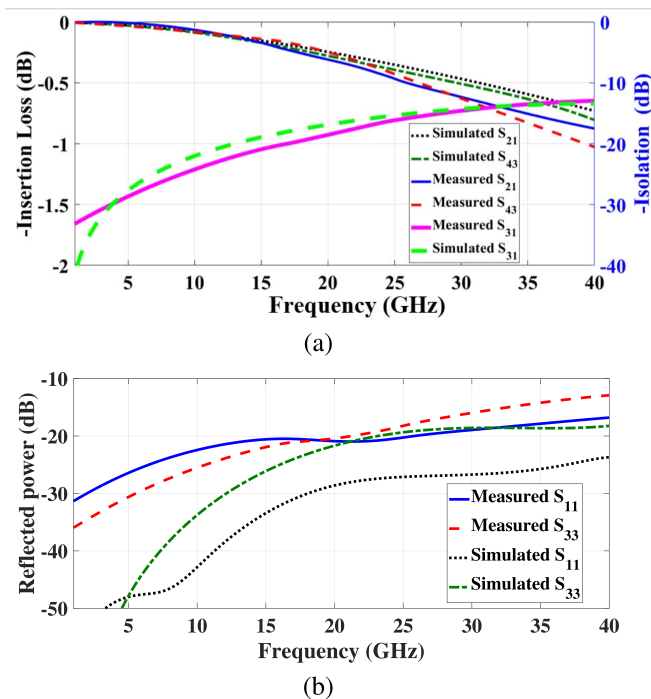

Fig. 6. Comparison of simulated and measured. (a) Insertion loss and isolation. (b) Reflected power of the proposed crossover device.

respectively. However, limited by the design rules of the low-cost PCB fabrications, G3 is changed to 150 μm, which is the least possible value of the gap.

The whole structure is simulated in HFSS. The simulated S-parameters are shown in Fig. 6. It is seen that the 10-dB impedance bandwidth ranges from dc to 40 GHz. The maximum insertion loss at 40 GHz is less than 0.75 dB for both paths.

To measure the S-parameters of this structure, microstrip lines were extended and tapered to attach K-type connectors. The effective area of the crossover is only 3 mm $\times$ 3 mm. The measured S-parameters of this circuit after deembedding the connector and microstrip line loss are shown in Fig. 6, which are in very good agreement with simulation. The measured insertion loss and return loss at the center frequency (20 GHz) are 0.35 and 21 dB, respectively. The measured port isolation (S_{31}) is around 19 dB.

TABLE I

SIMULATED AND MEASURED PERFORMANCE OF THE DESIGNED CROSSOVER IN DIFFERENT FREQUENCY BANDS

Frequency (GHz)	Insertion loss (dB)		Isolation (dB)		Return loss (dB)	
	Sim	Meas.	Sim	Meas.	Sim	Meas.
5	0.03	0.04	28	29	47	28
15	0.17	0.2	19	22	26	22
25	0.4	0.47	15	17	19	18
35	0.63	0.83	14	14	19	14

TABLE II

COMPARISON OF THIS LETTER WITH SIMILAR CROSSOVERS STRUCTURES

Structure	[5]	[6]	[7]	[9]	This work
size(mm)	15×15	8×15	30×30	10×10	3×3
Bandwidth (GHz)	0.9-1.1	3.1-11	DC-6	DC-10	DC-40
Return loss (dB)	10	10	20	20	21
Insertion loss (dB)	1	1.1	1	1	0.35
Isolation (dB)	10	15	20	23	19

Table I summarizes the simulated and measured performance of this structure at 5, 15, 25, and 35 GHz. Table II compares the measured performance of the designed crossover at the center frequency, i.e., 20 GHz, with the similar work. It is seen that the proposed structure has the largest bandwidth as well as the lowest effective size and insertion loss.

IV. CONCLUSION

A compact and wideband single-layer crossover for dc to 40 GHz is proposed in this letter. The measured bandwidth is significantly higher than the similar work. Furthermore, low insertion loss and coupling between paths are the key advantages of this structure.

REFERENCES

[1] T.-S. Horng, "A rigorous study of microstrip crossovers and their possible improvements," *IEEE Trans. Microw. Theory Techn.*, vol. 42, no. 9, pp. 1802–1806, Sep. 1994.

[2] Y. C. Chiou, J. T. Kuo, and H. R. Lee, "Design of Compact Symmetric Four-Port Crossover Junction," *IEEE Microw. Wireless Compon. Lett.*, vol. 19, no. 9, pp. 545–547, Sep. 2009.

[3] J.-J. Yao, C. Lee, and S.-P. Yeo, "Microstrip branch-line couplers for crossover application," *IEEE Trans. Microw. Theory Techn.*, vol. 59, no. 1, pp. 87–92, Jan. 2011.

[4] C. W. Tang, K. C. Lin, and W. C. Chen, "Analysis and design of compact and wide-passband planar crossovers," *IEEE Trans. Microw. Theory Techn.*, vol. 62, no. 12, pp. 2975–2982, Dec. 2014.

[5] L. Markley and G. V. Eleftheriades, "An ultra-compact microstrip crossover inspired by contra-directional even and odd mode propagation," *IEEE Microw. Wireless Compon. Lett.*, vol. 24, no. 7, pp. 436–438, Jul. 2014.

[6] A. Abbosh, S. Ibrahim, and M. Karim, "Ultra-wideband crossover using microstrip-to-coplanar waveguide transitions," *IEEE Microw. Wireless Compon. Lett.*, vol. 22, no. 10, pp. 500–502, Oct. 2012.

[7] W. Liu, Z. Zhang, Z. Feng, and M. Iskander, "A compact wideband microstrip crossover," *IEEE Microw. Wireless Compon. Lett.*, vol. 22, no. 5, pp. 254–256, May 2012.

[8] M. Fakharzadeh and S. Jafarlou, "A broadband low-loss 60 GHz die to rectangular waveguide transition," *IEEE Microw. Wireless Compon. Lett.*, vol. 25, no. 6, pp. 370–372, Jun. 2015.

[9] S. Y. Eom, A. Batgerel, and L. Minz, "Compact broadband microstrip crossover with isolation improvement and phase compensation," *IEEE Microw. Wireless Compon. Lett.*, vol. 24, no. 7, pp. 481–483, Jul. 2014.